ELSEVIER

Journal of Nuclear Materials 278 (2000) 96–103

journal of nuclear materials

www.elsevier.nl/locate/jnucmat

Evaluation of thermal aging embrittlement in CF8 duplex stainless steel by small punch test

Jin Sik Cheon[a,*], In Sup Kim[b]

[a] *Korea Heavy Industries and Construction Co. Ltd., 555 Guygok-dong Changwon 641-792, South Korea*
[b] *Korea Advanced Institute of Science and Technology, 373-1 Kusong-dong Yusong-gu Taejon 305-701, South Korea*

Received 8 June 1999; accepted 7 August 1999

Abstract

Small punch test was performed on CF8 duplex stainless steel aged at 370 and 400°C for up to 5000 h to characterize thermal aging embrittlement. At room temperature, the small punch (SP) load–displacement curve was similar in shape to those of ferritic steels and exhibited a good reproducibility in spite of ferrite–austenite structure. As the test temperature was lowered to a certain temperature depending on the degree of aging, the SP load showed a sudden drop followed by curve serration before the SP specimen fractured, resulting from the cracking of ferrite phase. While the aging heat treatment led to a slight increase of the yield strength, the transition appearing in the SP energy versus temperature curves shifted to higher temperature due to the hardening of ferrite phase. Additionally, phase boundary separation was an important factor in the degradation of the steel aged at 400°C.

1. Introduction

Duplex stainless steels, consisting of a duplex structure of austenite and ferrite, are widely used for critical components of primary water coolant system in nuclear power plant due to high strength, sound castability, and high resistance to stress corrosion cracking. Superior properties originate from the presence of ferrite, but the steels are degraded due to the formation of several phases within ferrite when they are aged in the temperature range from 280°C to 500°C. The degradation is called 'thermal aging embrittlement' [1].

There have been various methods by which the degree of thermal aging embrittlement can be evaluated. These methods are based on the variation in magnetic [2], chemical [3] or ultrasonic properties [4] due to microstructural changes during thermal aging. However, signals obtained from the physical property measurement are expected to be relatively weak. Moreover, material-specific correlation should be developed under particular testing environment. Another method, the measurement of the ferrite hardness, also has limitations in that the hardness change does not reflect the effects of ferrite content and distribution, and that the hardness continues to increase even in the case that the room-temperature Charpy energy shows full embrittlement after a certain period [5].

In comparison, small punch (SP) test method was developed recently to estimate mechanical properties by the direct fracture of a smaller specimen. The SP test has been reported to achieve successful results for evaluating mechanical properties such as yield strength [6], ductile-to-brittle transition temperature [7], and fracture toughness [8]. The SP test was proposed by the authors as a technique to determine the extent of thermal aging embrittlement of a duplex stainless steel.

2. Experimental

2.1. Material preparation

The chemical composition of the material examined here is shown in Table 1 which corresponds to ASME

* Corresponding author. Tel.: +82-551 278 3697; fax: +82-551 278 8546.
E-mail address: jscheon@hanjung.co.kr (J.S. Cheon).

0022-3115/00/$ - see front matter
PII: S0022-3115(99)00213-5

Table 1
Chemical composition (in wt%) of CF8 duplex stainless steel

C	Si	Mn	P	S	Ni	Cr	Mo
0.057	1.34	0.62	0.003	0.002	8.23	19.94	0.21

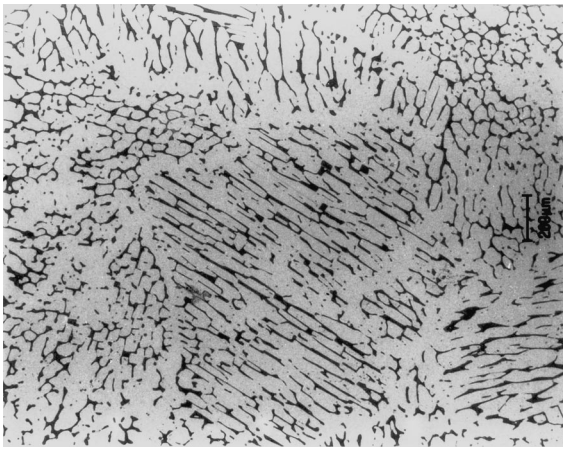

Fig. 1. Ferrite morphology of CF8 duplex stainless steel.

SA351 CF8 specification. The material was prepared by laboratory-scale vacuum induction melting. The aging treatments were performed at 370°C for 1500 and 3000 h, and at 400°C for 2500 and 5000 h [9]. The ferrite content of unaged material was 13% and decreased slightly with aging. The microstructure of duplex stainless steel was examined using optical microscope. As shown in Fig. 1, ferrite phase (black color) is embedded in austenite phase (gray color), forming an interlaced network. The spacing of ferrite phase is rather uniform but the orientation is not. It is also seen that some links of several ferrite phases continue over 1 mm without a break. The Vickers microhardness of the ferrite phase was measured with a load of 50 g, and the results are listed in Table 2 for each aging condition. Table 2 shows that hardness increase with increasing temperature and increasing time at a temperature.

2.2. SP test procedure

The dimensions of SP specimens were $10\times10\times0.5$ mm^3, and they were polished to 600 grit. The specimen thickness was controlled within ±10 μm and was measured using a digital micrometer with 1 μm resolution. The SP jig used in this study is schematically shown in Fig. 2(a). It consists of a 2.4 mm diameter punch, a 2.4 mm diameter ball, upper die, and lower die with a hole 4 mm in diameter. As load is applied to the SP specimen by the ball through the punch, the specimen is displaced into the lower die. The punch is instrumented to a load cell to measure the applied force. The upper die plays a role of guiding the punch and the ball. SP specimen is placed on the lower die and clamped between the upper and lower dies by four clamping screws. The specimen position and its support are illustrated in detail in Fig. 2(b). The error in the centering of the SP specimen within the jig was acceptably small. The punch was made by brazing a drilling pin into a tool steel piece. The lower die was designed to handle the specimen easily. An Instron 4204 was used for SP tests. The tests were conducted at a crosshead speed of 0.5 mm/min with a load cell of 5 kN capacity. The displacement was measured by detecting the crosshead motion. From 0°C to −100°C, the SP test jig was immersed in the ethanol-contained bath to which liquid nitrogen was slowly added to maintain test temperature. Below −100°C, the specimen temperature was sustained by controlling the heat conduction. During the tests, the temperature was monitored by K-type thermocouple placed close to the specimen through a small hole in the lower die and was controlled within ±2°C.

3. Results

3.1. SP load–displacement curve of duplex stainless steel

Fig. 3(a) shows the SP load–displacement curves obtained at room temperature with the unaged specimens of CF8 duplex stainless steel. The five curves well coincided with each other and the overall shape was like that obtained from the SP test on ferritic steels. With increasing degree of aging, the SP load tended to increase slightly at the same displacement as shown in Fig. 3(b).

SP load–displacement curves at various temperatures for unaged specimens are illustrated in Fig. 4(a). Above

Table 2
Microhardness of ferrite phase and yield strength of the steel for various aging conditions

Aging conditions	Unaged	370°C/1500 h	370°C/3000 h	400°C/2500 h	400°C/5000 h
Microhardness (Hv50)	258 ± 11	304 ± 11	341 ± 15	394 ± 17	445 ± 12
Calculated yield strength [MPa]	316 ± 10	356 ± 26	337 ± 9	360 ± 18	376 ± 26

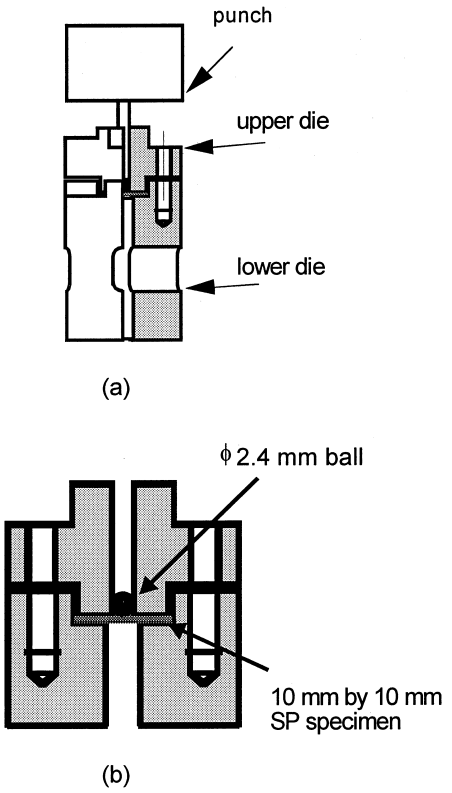

Fig. 2. Schematic drawing of the SP test apparatus: (a) overall configuration and (b) specimen positioning in the specimen support.

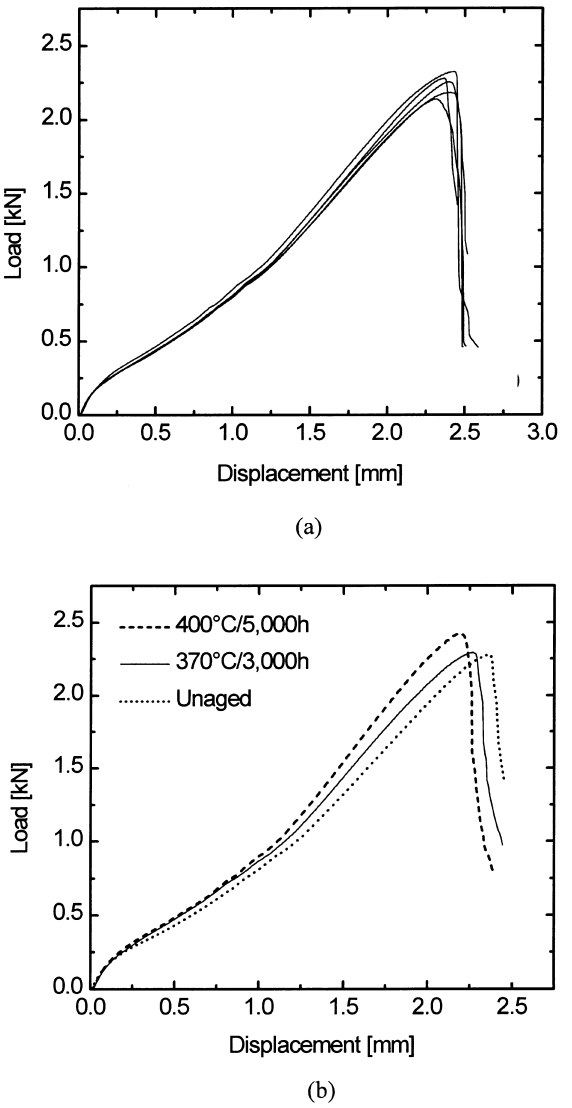

Fig. 3. Load versus displacement curves at room temperature for CF8 duplex stainless steel: (a) five unaged specimens and (b) three different conditions.

−150°C, the SP load exhibited a smooth decrease from the maximum load until the SP specimen broke with an abrupt load drop. As temperature is lowered below −150°C, there was a different load behavior in some tests. A sudden load drop initially occurred and then the load-displacement curve exhibited repeated rises and drops of load which persisted until the fracture of the SP specimen. Similar phenomena were observed in the set of load–displacement curves for aged conditions except with further aging the serrated curve developed at a higher temperature. It is also observed that the scattering of data in the region of ductile–brittle transition was remarkably larger than that of ferritic steels. As an example the load–displacement curves are plotted in Fig. 4(b) for the unaged SP specimen tested at −175°C. The largest value in the maximum SP load (3.54 kN) is much higher than that of others.

Some of the SP tests were interrupted and the surface appearance of the specimen was observed before and after the initial load drop. To distinguish ferrite from austenite, one surface of the unaged specimen was polished with 1 μm diamond paste and then electrolytically etched in 40 wt% KOH solution. Fig. 5 is the scanning electron micrographs of the unaged specimen tested at −175°C. Figs. 5(a) and (b) are SEM photographs of the SP specimen whose test was interrupted before the initial load drop. The figures reveal several small circumferential cracks that are preferentially formed in the ferrite phases located in the off-centered region of the specimen. SEM photographs of a different specimen taken just after the initial load drop are shown in Figs. 5(c) and (d). Fig. 5(c) illustrates that the crack propagates along the circumferential direction. The fracture surface was composed of the ductile dimple and cleavage as shown in Fig. 5(d).

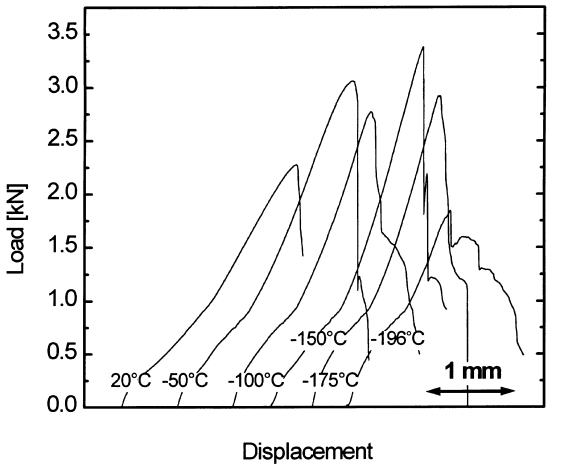

(a)

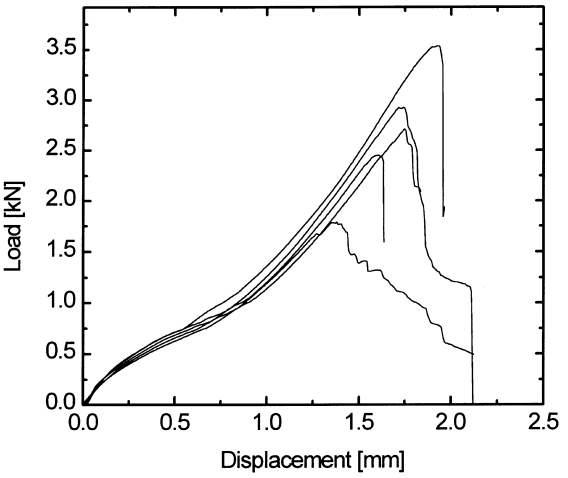

(b)

Fig. 4. Load versus displacement curves for unaged specimen: (a) at various test temperatures and (b) at −175°C.

3.2. Embrittlement of thermally aged duplex stainless steel

Based on the dependence of SP load–displacement curves on test temperature, the degree of thermal embrittlement was evaluated. The energy consumed during the test until failure, called SP energy, has been adopted to describe the temperature dependence of SP load–displacement curve. On the other hand, when the serrated load behavior appeared, the contributing energy beyond the initial load drop was commonly not included in the calculation of the SP energy [10,11].

The SP energy is plotted in Fig. 6 as a function of test temperature for unaged and aged specimens. As temperature decreased, the SP energy showed a transition, which has been correlated with the ductile-to-brittle transition temperature of the material [7]. Above the transition temperature, it was observed that SP specimens had a substantial deformation at failure. Fig. 6 also shows that aging treatment resulted in a shift to higher transition temperature and the amount of the shift was larger in the specimen aged at higher temperature. At the constant aging temperature, however, it was difficult to observe a distinct difference in the transition temperature with aging time.

The fracture surface of the SP specimen tested at room temperature was examined by SEM. Fig. 7 shows the fracture mode appreciably changed due to aging although the aging heat-treatment led to a slight variation in the SP load–displacement curves at room temperature (Fig. 3(b)). The unaged specimen and the specimen aged at 370°C for 3000 h consisted of ductile failure and dimpled ductile tearing on their fracture surface. The dimple size of the 370°C/3000 h aged specimen was smaller than that of the unaged specimen and the depth was shallower. For the specimen aged at 400°C for 5000 h, however, the fracture surface contained a significant amount of separation of the ferrite–austenite phase boundary with a little cleavage of ferrite phase as well as ductile failure.

4. Discussion

4.1. Role of ferrite in the SP load behavior

Some SP specimens under current investigation showed the initial load drop and curve serration on the load–displacement curve at low temperature. For ferritic steels, this kind of load drop was reported in the SP test on very brittle phosphorous–copper doped steels [11] and disk bend test on cross-notched specimen [10]. In these investigations, cracks were easily formed due to weak grain boundary where phosphorous atoms are segregated and due to notch where stress is intensified, respectively. Similarly, ferrite phase in the present steel gave a good circumstance for crack initiation as temperature decreased. Several small cracks were generated at the ferrite phases located at the edge of the contact region between the SP ball and the specimen, as shown in Fig. 5. The crack initiation in the off-centered region is related to the deformation state. During the SP test, the SP specimen experiences various deformation states with proceeding deformation [12]. It is thought that the deformation regime at the initial load drop corresponds to the membrane stretching. In the membrane stretching regime, the strain is concentrated circumferentially at the edge of contact region because of the large friction on the contact surface between the ball and the specimen and small clearance of the ball and the die hole [13]. Moreover, the stretching condition may become similar

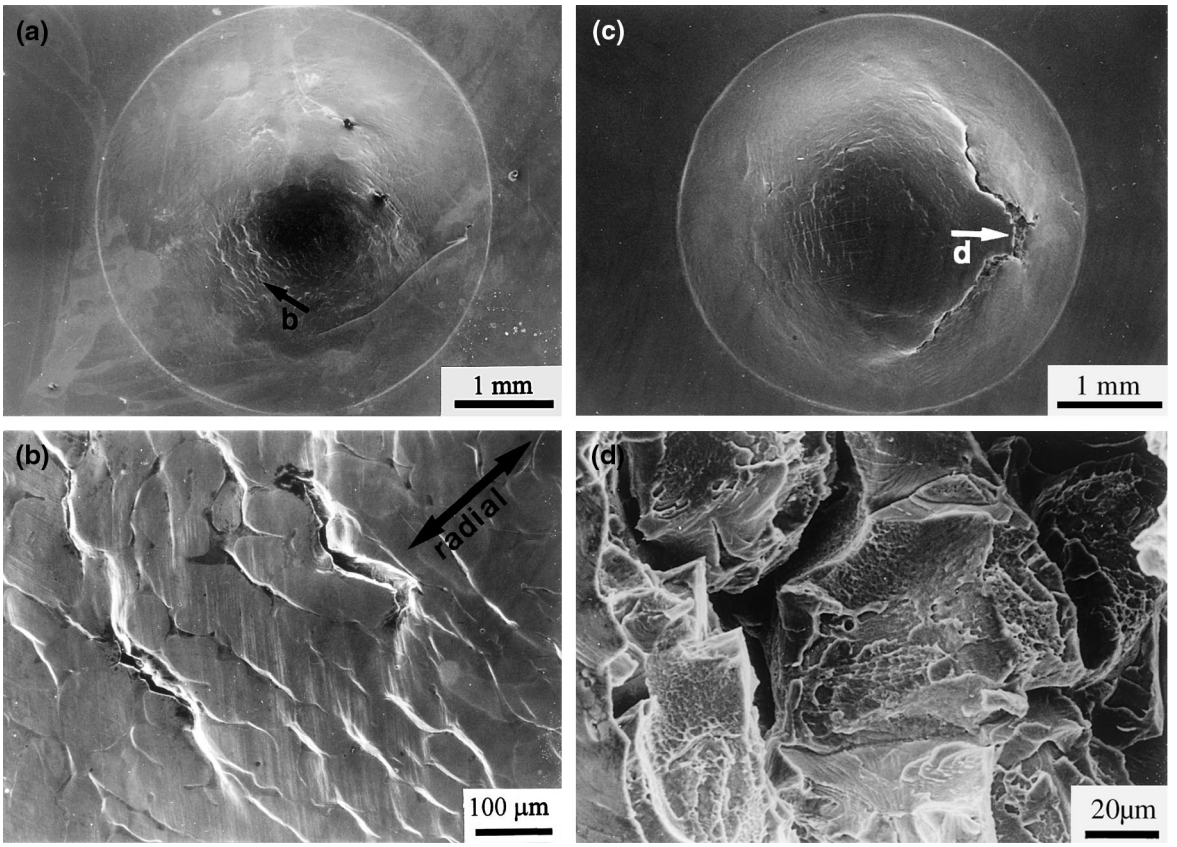

Fig. 5. Scanning electron micrographs of unaged specimen tested at −175°C: (a) overall appearance of the SP specimen interrupted before the initial load drop; (b) is higher magnification of the regions indicated in (a); (c) overall appearance of the SP specimen after abrupt load drop and (d) fracture surface on the regions indicated in (c).

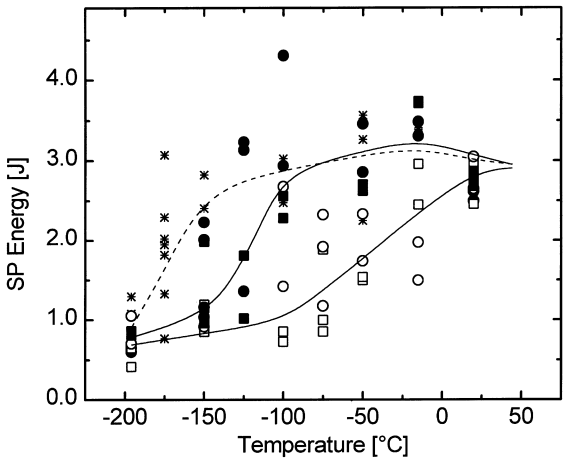

Fig. 6. SP energy transition curves for CF8 duplex stainless steel (★: Unaged, ■: 370°C/1500 h,●: 370°C/3000 h, □: 400°C/2500 h, and ○: 400°C/5000 h. Three curves represent the effect of aging temperature irrespective of aging time.).

to a plane strain stretching [14] under which the radial stress component is twice as high as the circumferential stress component [15]. Thus, the circumferential ferrite in the region is easily fractured by the radial stress. Immediately, the small cracks initiated at the ferrite are arrested by ductile austenite. As further deformation proceeds, the cracks are combined with each other by the tearing of surrounding austenite phase as the fracture mechanism of cast duplex stainless steel [1,16]. The cleavage and ductile dimple in Fig. 5(d) supports this conclusion. Consequently, by associating the SEM micrographs with the load–displacement curves, it is believed that the initial load drop is attributed to the long crack formed by the connection of small cracks. The subsequent increase in the load can be explained by the previous discussion that further load is required to bend the cracked SP specimen [10] and to maintain the same stress level within the specimen due to the increase of contact area as well as the effect of work hardening [7].

Another notable characteristic of the SP test with the duplex stainless steel is the large scatter of the data

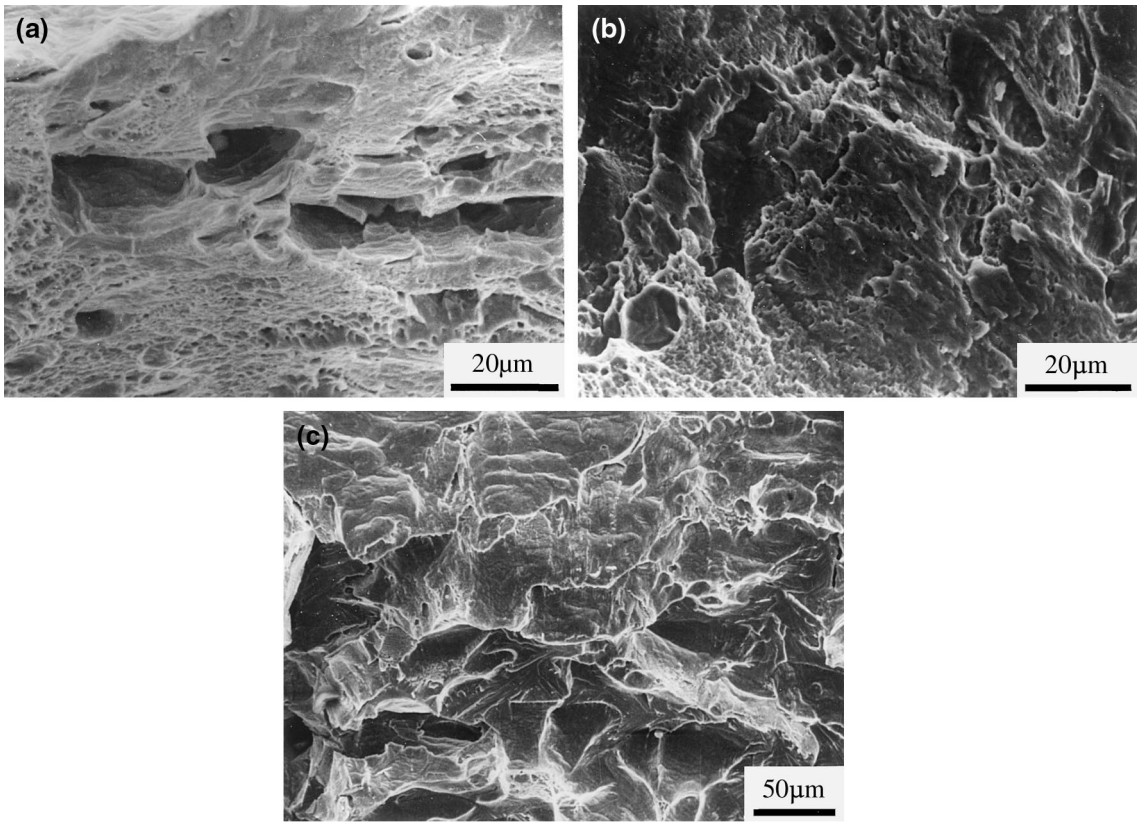

Fig. 7. Scanning electron micrographs of the fracture surface for unaged and aged specimens tested at room temperature: (a) unaged; (b) 370°C/3000 h, and (c) 400°C/5000 h.

in the transition temperature range as shown in Fig. 4(b) and Fig. 6. The scattering was much larger than that observed in the SP test of ferritic steels. At low temperature, such a scattering behavior is observed in Charpy V-notch (CVN) and fracture toughness tests of ferritic steel. This is related to the fact that strength of brittle material like a body-centered-cubic metal at low temperature is determined by the single-most susceptible flaw rather than by an average volume of the distribution of flaws [17]. Further, the scatter becomes larger as the specimen size decreases. Thus it is unavoidable that the SP data exhibit significant scatter in the transition temperature range. In addition to the inherent characteristics of ferrite at low temperature, the severe variation in the SP data of the duplex stainless steel is thought to be associated with the preference of cracks at the ferrite phase. SEM observations of the specimen with the maximum SP load of 3.54 kN at −175°C show that the ferrites in the edge of the contact area are not densely distributed and not large enough to induce the interconnection of neighbor cracks (Fig. 8(b)) or their orientation is mostly radial which is unfavorable to crack initiation as discussed early (Fig. 8(c)). Hence crack initiation is difficult and the propagation of the crack generated at the ferrite phases would deviate from the circumferential direction which requires extremely high load to occur the fracture of the specimen.

4.2. SP test for the evaluation of thermal aging embrittlement

The aging treatment increased the ferrite hardness markedly and the load response to displacement became somewhat rapid. The effect of the hardening on the strength was quantified in terms of yield strength, which was correlated with the load at the breakaway from the initial linearity of load–displacement curve as shown in Fig. 3(b). The calculated yield strength is given in Table 2. The effect of aging on the yield strength at room temperature was minor, while microhardness of the ferrite increased about twice in the specimen aged at 400°C for 5000 h. It is thought that the small hardening was attained due to the small content of ferrite phase and the constant microhardness of austenite phase (about 200 HV).

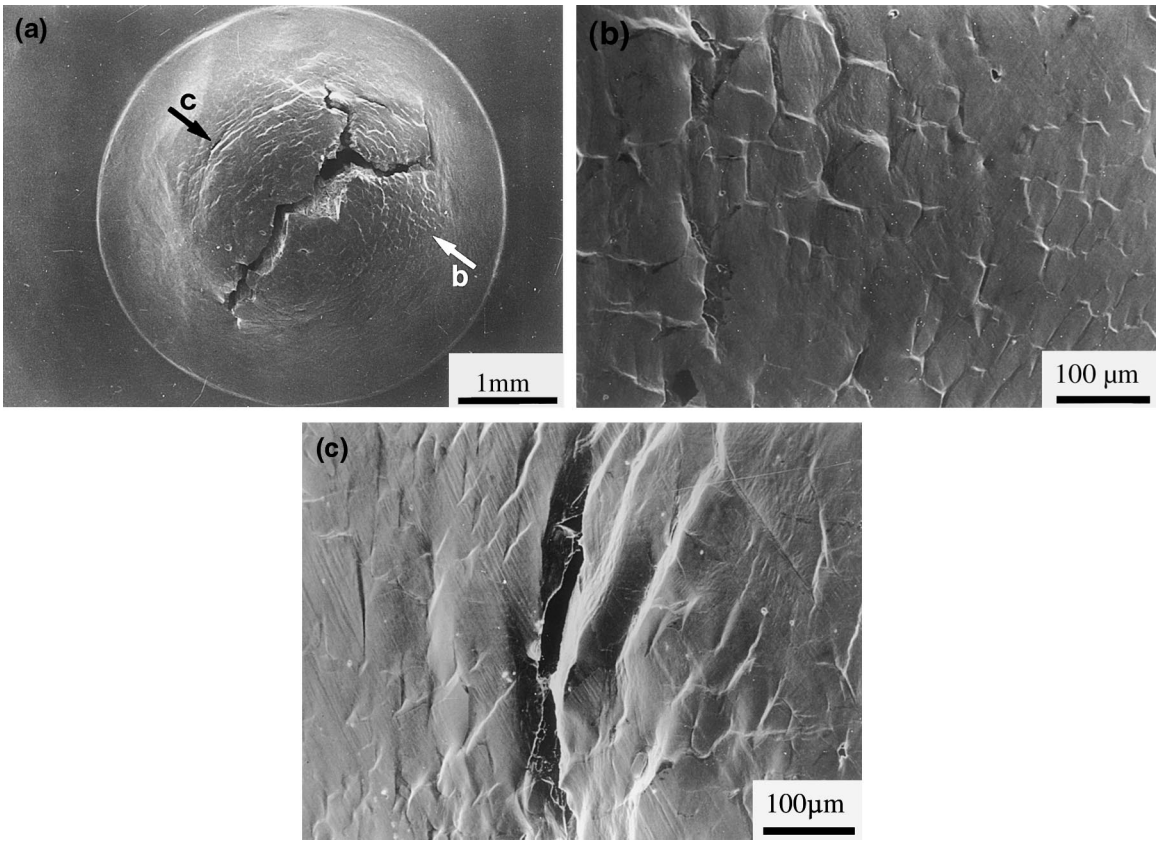

Fig. 8. Scanning electron micrographs of unaged specimen fractured at 3.54 kN: (a) overall appearance, (b); and (c) are higher magnification of the regions indicated in (a).

In contrast to the results of the yield strength, the aging treatment gave a significant influence on the variation of the SP energy with temperature. Considering the preference of cracks at ferrite phase and the invariance of austenite hardness during aging, the shift in the transition temperature is attributable to the hardening of ferrite phase. The embrittlement of ferrite phase is caused because dislocations are impeded by compositional fluctuations arising from spinodal decomposition and precipitation of the G phase [18,19]. In addition, carbide precipitation at the ferrite–austenite interface is considered to be a secondary degradation mechanism for the 400°C aged condition of the current steel. In Fig. 7, the specimen aged at 400°C for 5000 h exhibited different fracture mode clearly distinguished from the ductile failure and dimpled ductile tearing which appeared on the specimens aged below 400°C. In the same steel, the carbides were not observed in the unaged condition but precipitated at ferrite–austenite boundaries in the specimen aged at 400°C for 7000 h [9]. The precipitation of phase boundary carbide significantly occurred at 400°C or 450°C for CF8 heats containing carbon content more than 0.05 wt% and controlled the fracture mode [18]. Hence, the carbon content of the present steel (0.057 wt%) and carbide precipitation explain the ferrite–austenite boundary separation took place in the 400°C aged specimen.

While the effect of aging temperature on the shift of the transition temperature was manifested, distinctive difference in proportion to aging time was not seen by the SP test method. This limitation, however, is not peculiar in SP test but also appeared in CVN test although the CVN test is likely to magnify the difference in the degree of aging due to high strain rate and triaxial stress state in comparison with the SP test [20]. It seems that the minor microstructural change caused by the relatively small difference in aging time may not be identified. Furthermore, it was reported that the embrittlement became saturated after aging for 2500 h at 400°C [1].

No attempt was made to correlate the present results to the behavior of the full Charpy energy curve because of specimen availability. However, it is believed that the SP test method is quite appropriate for estimating the degree of embrittlement of duplex stainless steel in comparison with the other methods mentioned in

Section 1. Besides, as most stainless weld metals of the AISI/AWS 300 series have a duplex austenitic–ferritic microstructure in an as-welded condition [21] and are considerably degraded in the toughness during long-term aging [22], the toughness evaluation of the stainless weldments could be achieved by the SP test technique.

5. Conclusions

Thermal aging embrittlement of CF8 duplex stainless steel has been investigated using the small punch test. The material was aged at 370°C and 400°C up to 5000 h. The results obtained are as follows:

(1) At room temperature, the general trend and reproducibility of the SP load–displacement curves were similar to those of ferritic steels. Decreasing test temperature led to a sudden load drop and curve serration in the SP load which are thought to be related to the preference of the cracks initiation at ferrite phases.

(2) With increasing the degree of aging, the yield strength tended to increase to some extent. The variation of the SP energy with temperature exhibited a transition which was shifted as a result of aging treatment, and the amount of the shift was larger in the specimen aged at higher temperature, which is in good agreement with the change in fracture mode.

References

[1] O.K. Chopra, A. Sather, Initial assessment of the mechanisms and significance of low-temperature embrittlement of cast stainless steels in LWR systems, US Nuclear Regulatory Commission Report, NUREG/CR-5385, Argonne National Laboratory, 1990.
[2] S. Evanson, M. Otaka, K. Hasegawa, J. Eng. Mat. and Tech. 114 (1992) 41.
[3] J.S. Park, Y.K. Yoon, Scripta Metall. 32 (1995) 1163.
[4] S. Matsubara et al., in: A. Rao, R. Duffey, D. Elias (Eds.), Proceedings of the Fourth International Conference on Nuclear Engineering, American Society of Mechanical Engineers, New Orleans, USA, 10–14 March 1996, p. 215.
[5] J.J. Shiao, C.H. Tsai, J.J. Kai, J.H. Huang, The Minerals, Metals & Materials Society, in: R.E. Gold, E.P. Simonen (Eds.), Proceedings of the sixth International Symposium on Environmental Degradation of Materials in Nuclear Power Systems, San Diego, 1–5 August 1993, p. 391.
[6] J.S. Cheon, I.S. Kim, J. Testing Eval. 24 (1996) 255.
[7] J.M. Baik, J. Kameda, O. Buck, Scripta Metall. 17 (1983) 1443.
[8] J.R. Foulds et al., J. Testing Eval. 23 (1995) 3.
[9] J.S. Park, KAIST, PhD thesis (in Korean), 1995.
[10] J. Kameda, X. Mao, J. Mater. Sci. 27 (1992) 983.
[11] G. Koshe, M. Ames, O.K. Harling, J. Nucl. Mater. 141–143 (1986) 513.
[12] M.P. Manahan, Nucl. Technol 63 (1983) 295.
[13] X. Mao, T. Shoji, H. Takahashi, J. Testing Eval. 15 (1987) 30.
[14] Jitsukawa et al., in: W.R. Corwin, F.M. Haggag, W.L. Server (Eds.), Small Specimen Test Technique Applied to Nuclear Reactor Vessel Thermal Annealing and Plant Life Extension, ASTM STP 1204, 1993, p. 289.
[15] W.A. Backofen, Deformation Processing, Addison-Wesley, Massachusetts, 1972.
[16] E.L. Brown, T.A. Whipple, R.L. Tobler, Metall. Trans. A 14A (1983) 1179.
[17] G.E. Dieter, Mechanical Metallurgy, McGraw-Hill, London, 1988.
[18] H.M. Chung, Int. J. Pres. Ves. and Piping. 50 (1992) 179.
[19] P.H. Pumphrey, K.N. Akhurst, Mater. Sci. Technol. 6 (1990) 211.
[20] P. McConnell, W. Sheckherd, D. Norris, J. Mater. Eng. 11 (1989) 227.
[21] T. Takalo, N. Suutala, T. Moisio, Metall. Trans. A 10A (1979) 1173.
[22] D.J. Alexander, R.K. Nanstad, The effects of aging for 50,000 h at 343°C on the mechanical properties of type 308 stainless steel weldments, Oak Ridge National Laboratory, CONF-9508166, 1995.